Interspecies comparison of plasma metabolism and sample stabilization for quantitative bioanalyses: Application to (R)-CE3F4 in preclinical development, including metabolite identification by high-resolution mass spectrometry

Balthazar Toussaint, Hervé Hillaireau, Emmanuel Jaccoulet, Catherine Cailleau, Pauline Legrand, Yves Ambroise, Elias Fattal

Interspecies comparison of plasma metabolism and sample stabilization for quantitative bioanalyses: application to (*R*)-CE3F4 in preclinical development, including metabolite identification by high-resolution mass spectrometry

Balthazar Toussaint[1,2], Hervé Hillaireau[1], Emmanuel Jaccoulet[1,3], Catherine Cailleau[1], Pauline Legrand[2,4], Yves Ambroise[5], Elias Fattal[1]

[1] Université Paris-Saclay, CNRS, Institut Galien Paris Sud, 92296, Châtenay-Malabry, France.

[2] Département de Recherche et Développement Pharmaceutique, Agence Générale des Équipements et Produits de Santé (AGEPS), Assistance Publique des Hôpitaux de Paris (AP-HP), Paris, France.

[3] Hôpital européen Georges Pompidou (HEGP), Service Pharmacie (AP-HP), Paris, France.

[4] Université de Paris, Faculté de sciences pharmaceutiques et biologiques, Unité de Technologies Chimiques et Biologiques pour la Santé (UTCBS), CNRS UMR8258, Inserm U1022, Paris, France.

[5] Université Paris-Saclay, CEA, Institut des Sciences du Vivant Frederic Joliot, 91191, Gif-sur-Yvette, France.

*Corresponding Author:
Elias Fattal, Ph.D
Université Paris-Saclay
Institut Galien Paris-Sud
UMR CNRS 8612
5 Rue Jean-Baptiste Clément
92290 Châtenay-Malabry
France

Abstract

The CE3F4 is an inhibitor of the type 1 exchange protein directly activated by cAMP (EPAC1), which is involved in numerous signaling pathways. The inhibition of EPAC1 shows promising results *in vitro* and *in vivo* in different cardiac pathological situations like hypertrophic signaling, contributing to heart failure, or arrhythmia. An HPLC-UV method with a simple and fast sample treatment allowed the quantification of (*R*)-CE3F4. Sample treatment consisted of simple protein precipitation with 50 µL of ethanol and 150 µL of acetonitrile for a 50 µL biological sample. Two wavelengths were used according to the origin of plasma (220 or 250 nm for human samples and 250 nm for murine samples). Accuracy profile was evaluated for both wavelengths, and the method was in agreement with the criteria given by the EMA in the guideline for bioanalytical method validation for human and mouse plasma samples. The run time was 12 min allowing the detection of the (*R*)-CE3F4 and a metabolite. This study further permitted understanding the behavior of CE3F4 in plasma by highlighting an important difference between humans and rodents on plasma metabolism and may impact future *in vivo* studies related to this molecule and translation of results between animal models and humans. Using paraoxon as a metabolism inhibitor was crucial for the stabilization of (*R*)-CE3F4 in murine samples. HPLC-UV and HPLC-MS/MS studies were conducted to confirm metabolite structure and consequently, the main metabolic pathway in murine plasma.

Keywords: EPAC1, High-performance liquid chromatography, Species metabolism, Validation method, Plasma stability study

1 Introduction

Heart disease is one of the major issues of the last century which burden remains significant with high morbidity and mortality that has not been improved by any treatment modality [1]. Many efforts are performed to find new efficient drugs in the cardiology field. Very recently, one *in vivo* study described the potential of a new drug, CE3F4, on C57BL/6 mouse models for atrial/ventricular arrhythmias [2]. CE3F4 is a tetrahydroquinoline analog identified as a specific and uncompetitive inhibitor of EPAC1 (exchange protein directly activated by cAMP 1) [3,4]. The downregulation of EPAC1 activity can restore or protect physiological functions, which could be exploited for new treatments of heart failure [5] and arrhythmia [2,6]. CE3F4 has demonstrated *in vitro* efficient inhibition of cellular mechanisms involving EPAC1 in pathological cardiac conditions [7–9]. Moreover, other diseases such as breast, gastric, and pancreatic cancers [10–12], Alzheimer's disease [13], and depression [14] may benefit from CE3F4. Altogether, these results were promising for further pharmaceutical development of this drug.

Extensive and comprehensive preclinical studies are required to yield toxicological, pharmacokinetic, and pharmacological information before clinical trials of a new drug [15]. Typically, pharmacokinetic/pharmacodynamic (PK/PD) study involves *in vitro* analysis from animals (e.g. rodents) and human plasma [16]. Quantitative analysis is of utmost importance for this purpose [16,17]. However, particular care should be taken in analytical strategies due to metabolism differences between species. To facilitate the preclinical results to clinical study transposition, drug metabolism should be performed *in vitro* with murine and human plasma at an early stage of development. This raises the challenge of the analysis in a complex medium such as plasma, containing various degrading enzymes that differ from species. Indeed, it is noteworthy that differences in the type of enzyme existing between mammalian species may impact drug analysis and subsequently lead to considerable challenges in interpreting the data. Interspecies differences in drug metabolism were reported between rodents and humans [18–20]. For example, carboxylesterases, which are known to degrade drugs containing amides, carbamate, esters, or thioesters bonds [21,22], are present in rodent plasma but not in human plasma [23]. Therefore, plasma metabolism can lead to drug degradation during sample collection, preparation, or storage [24], inducing a false estimate of the drug level in plasma which is detrimental for monitoring purposes [25]. To overcome these issues, several procedures are currently used for *ex vivo* drug stabilization before

analysis. To achieve drug stabilization in plasma samples, specific enzyme inhibitors, involved in the degradation, have been described such as irreversible non-competitive inhibitors like pesticides inhibiting esterases to stabilize diformyldapsone [19], oseltamivir [25], and zeylenone [26]. Other inhibitors like tetrahydrouridine demonstrated an interest in gemcitabine stabilization (competitive inhibitor) before quantification [27], or EDTA (ethylenediaminetetraacetic acid) which can be used to inhibit metal-dependent enzymes [28,29]. Less-specific methods can be used such as cold temperature to slow-down enzymatic reaction kinetic, pH setting outside optimal range for enzyme activity [30], or protein precipitation by organic solvent [31,32], this latest method presenting the advantage to deproteinize the plasma sample making it suitable for analysis. Very recently, different methods were combined to stabilize molecules of interest in plasma before analysis, as EDTA with sample acidification and refrigerated conditions for osimertinib stabilization [33], or sodium fluoride (esterase inhibitor) associated to sample acidification, EDTA, derivatization, and refrigerated conditions for the simultaneous quantification of vicagrel and its two metabolites [34].

Nevertheless, when it comes to a new drug, the enzymes likely to affect the clearance of the drug are not always identified. Di *et al.* [35] emphasized the importance of plasma stability experiments on hydrolyzable drugs during drug discovery, as this type of study is very informative about compound screening, drug liability, and the potential need to use hydrolase inhibitors during PK studies [35]. In the case of (*R*)-CE3F4, to the best of our knowledge, no degrading enzyme in plasma has yet been reported. To conduct PK/PD studies, the behavior of (*R*)-CE3F4 in blood or plasma medium (e.g. differences in pharmacokinetics, metabolism) should be conducted [36,37]. CE3F4 shows a N-formamide function (**Fig. 1**), and thus, has the potential to be inactivated by hydrolases, including esterases or N-formamidase [18–20]. Due to the known differences between humans and rodents in the expression of the wide class of hydrolases [23,38,39], a specific approach must be considered.

The present paper describes the first method for (*R*)-CE3F4 quantification in both human and mouse plasma using LC-UV system. The method included enzyme inhibition, extraction, and assay steps. The method was validated through the European Medicine Agency guideline for bioanalytical analysis, on two wavelengths (220 and 250 nm) to overcome a lack of specificity depending on the origin of the plasma matrices analyzed (i.e. human or mouse). It

was then applied to plasma samples, and an essential difference in plasma metabolism has been highlighted *ex vivo* between murine and human plasma.

2 Materials and methods

2.1 Chemicals

A racemic mixture of CE3F4 and the deformylated-CE3F4 were synthesized using published procedures [40]. The active enantiomer (*R*)-CE3F4 was isolated with a purity >99% and enantiomeric excess (ee) >98% by applying the racemic mixture to a 250 × 30 mm Chiralpak® IB column (Daicel Corporation, Japan) equilibrated with n-hexane/propan-2-ol (95/5) at 42 mL/min. Paraoxon-ethyl (paraoxon) with the standard analytical grade, ethylenediaminetetraacetic acid disodium salt dihydrate (EDTA) with purity >99%, benzil with purity >98%, and bis(4-nitrophenyl) phosphate (BNPP) with purity >99%, polyethylene glycol 200 Da (PEG_{200}), Solutol® HS 15, phosphate-buffered saline (PBS) at pH 7.4 (sterile and suitable for cell culture) were acquired from Sigma-Aldrich (Saint-Louis, MO, USA). L-α-phosphatidylcholine from egg (EggPC), 1,2-distearoyl-sn-glycero-3-phosphoethanolamine-N-[methoxy(polyethyleneglycol)-2000] ($DSPE\text{-}PEG_{2000}$) were obtained from Avanti. Miglyol® 812 was purchased from Sasol (Johannesburg, South Africa). Zoletil® 50 (tiletamine, zolazepam), Rompun® 2% (Xylazine), Iso-Vet (isoflurane) were respectively purchased from Virbac (Carros, France), Bayer (Leverkusen, NRW, Germany), and Piramal Critical Care (Voorschoten, Netherlands). Ethanol (EtOH), as well as dimethyl sulfoxide (DMSO), were bought from VWR (Radnor, PA, USA), acetonitrile (ACN) with HPLC grade was purchased from Carlo Erba Reagents (Val-de-Reuil, France). Deionized water (H_2O) was produced by a Milli-Q water purifying system (Millipore, Milford, MA, USA). For the LC-MS experiment, water, acetonitrile, and formic acid were acquired from Merck KGaA (Darmstadt, Germany).

2.2 Biological samples

Human blank plasmas were obtained from blood donations from healthy volunteers who signed written informed consent (French Blood Establishment, La Plaine Saint-Denis, France). A sampling of murine plasmas was carried out according to the ethical committee (agreement number APAFIS#5584-20 16050312271349 v4). Blood samples were collected in heparinized tubes. After centrifugation at 500 g for 10 minutes in polypropylene tubes, plasmas were separated from the pellets and stored at -20°C.

2.3 Preparation of (R)-CE3F4 stock solutions, calibration standards, and quality controls

All liquids were handled with MICROMAN E positive displacement pipettes (Middleton, WI, USA) due to the viscosity of plasma samples and the use of organic solvents. Two stock solutions of (*R*)-CE3F4 were prepared in ethanol at a concentration of 1000 µg/mL, for calibration, and quality controls (QC). They were stored at +5°C. For the preparation of calibration standards, serial dilution (dilution factor = 2.43) in ethanol was performed from the stock solution to obtain an eight levels calibration curve with concentrations ranging from 0.40 to 200 µg/mL (**Table 1**). For the preparation of QC, appropriate volumes of stock solutions were evaporated to dryness at 40°C under a stream of nitrogen in 10 mL calibrated flasks for human QC or in 5 mL calibrated flasks for murine QC. For human QC, the dry residue was taken up with 10 mL of blank human plasma and mixed under magnetic stirring for two hours to obtain appropriate solubilization of the residue in the plasma at the six concentrations levels from 0.40 to 150 µg/mL (**Table 1**). For murine QC, 5 mL of mouse plasma loaded with paraoxon (final concentration of 10^{-4}M) were used to obtain three concentration levels of (*R*)-C3F4 (0.40, 8.00, and 150 µg/mL) (**Table 1**). These QC were defined as working solutions and were stored at -20°C.

2.4 Sample treatment

Using 2 mL polypropylene microcentrifuge tubes, 50 µL of calibration standards were added to 50 µL of (*R*)-CE3F4-free human plasma for the calibration samples and followed by a vortex-mixing step (10 seconds). For plasma samples spiked with (*R*)-CE3F4 (human plasma as QC for validation, human and murine plasmas for metabolism experiments), 50 µL of plasma was supplied with 50 µL of ethanol and followed by a vortex-mixing step (10 seconds). The proportions for each component (plasma, ethanol) were identical between calibration samples and QC (**Table 2**). Protein precipitation was performed by the addition of 150 µL of acetonitrile followed by a vortex-mixing for 10 seconds. After precipitation, tubes were centrifuged at 13,000 g for 10 minutes at room temperature, then 100 µL of the supernatant was collected into autosampler vials. 15 µL of the supernatant was injected into the chromatographic system.

2.5 Stock solutions of enzyme inhibitors

Several stock solutions of paraoxon, BNPP, and benzil were separately prepared at the concentration of 10^{-2} M, 10^{-3} M, and 10^{-4} M in DMSO. EDTA was solubilized in water to obtain a concentration of 200 mM.

2.6 Instruments

2.6.1 UV/Visible spectrophotometer

The UV absorbance spectra of (*R*)-CE3F4 were acquired using a Lambda 25 UV/VIS spectrometer from PerkinElmer (Waltham, MA, USA). The acquisition was performed with the software (UV WinLab from PerkinElmer) in scan mode from 195 to 400 nm with an acquisition rate of 480 nm/min, a slit width of 1 nm, and a data interval of 1 nm. Samples were analysed in a quartz cuvette (Hellma Analytics, Paris, France), and the optical pathlength was 10 mm. Appropriate dilutions of (*R*)-CE3F4 in ACN were performed to obtain 4.0, 8.0, and 16.0 µg/mL. After subtraction of the blank (ACN), absorbances at each wavelength have been divided by the corresponding concentration of the analysed sample to obtain the molar extinction coefficient.

Second derivate UV spectra were calculated using the Savitzky-Golay (SG) algorithm to identify UV maxima. Such a procedure highlights the potential wavelengths of interest for setting up chromatographic analysis. The convolution coefficients used were those to perform the SG second derivative with a quadratic/cubic polynomial fitting and a window size of nine points.

2.6.2 Liquid chromatography with UV detection

LC was performed on a Waters HPLC system (Milford, MA, USA) equipped with a diode array detector (Waters 2996 PDA), an injector (Waters 717 plus Autosampler), and a quaternary pump (Waters 600 HPLC pump). An external heater/chiller for the column was used (GRACE Model 7956R, Columbia, MD, USA). The separation was performed on XBridge C18 3.5 µm, 4.6 × 100 mm column (Waters). The oven temperature was set at 35°C. The mobile phase consisted of a mixture of water and acetonitrile (40:60, v/v) under isocratic mode at a flow rate of 1 ml/min. The acquisition was carried out from 194 to 400 nm with a resolution of 1.2 nm. Chromatograms were registered at 220 and 250 nm.

2.6.3 Liquid chromatography with MS/MS detection

Analysis was performed on RP-HPLC (ACQUITY, Waters, Manchester, UK) hyphenated to LTQ-orbitrap XL mass spectrometer (Thermo-Fischer Scientific, Les Ulis, France) specifically for identification purpose. The chromatographic conditions were very similar to the HPLC-UV method. Differences stood in the addition of formic acid 0.1% (v/v) into the mobile phase (water and ACN, 40:60, v/v) and in the flow rate which was set at 0.5 mL/min. The column remaining the same (XBridge C18 3.5 µm, 4.6 × 100 mm) was kept at the same temperature (35°C). Mass spectrometry analyses were conducted with a heated electrospray

ionization (ESI) interface (HESI-II) operating on positive mode with the following parameters: ESI voltage of +4.0 kV, sheath gas flow rate value of 80, and an auxiliary gas flow rate value of 12. Source heating temperature was set to 300°C, capillary and tube lens voltage to a value of 35 V and 90 V respectively. Mass/charge (m/z) range was 50-500. Full MS scans were recorded in profile mode using the high-resolution FTMS analyzer (R = 60,000). MS/MS fragmentation was performed by collision-induced dissociation (CID) using a normalized CID energy of 35. Data acquisition was controlled by Xcalibur software (Thermo-Fischer Scientific, Les Ulis, France).

2.7 Analytical method validation for (R)-CE3F4 plasma stability studies

The validation procedure was adapted from the European Medicine Agency (EMA) guideline for bioanalytical method validation which defines the acceptance criteria [41]. This procedure was carried out with plasma samples on three separate days, following the methodology from the *Société Française des Sciences et Techniques Pharmaceutiques* (SFSTP) previously reported [42–44]. LC-UV system has been used, and the signal was the chromatographic peak area at 220 nm and 250 nm.

2.7.1 Specificity

The specificity of this method was demonstrated by injecting the extracts blank plasma from 6 human or murine sources, the extracts of plasma spiked with other compounds like enzyme inhibitors (i.e. paraoxon, BNPP, benzil), or molecules which can be used for *in vivo* experiment as isoflurane, or the association Zoletil® (tiletamine, zolazepam) plus Rompun® (xylazine) at lethal dose. The specificity of the method was also explored regarding excipients which can be used for the formulation of the (*R*)-CE3F4 (PEG_{200}, Solutol HS 15, EggPC, DSPE-PEG_{2000}, Miglyol 812). No peak with a surface area equal to at least 20 % of the LLOQ should appear on the chromatogram under or near the (*R*)-CE3F4 (resolution $Rs < 1.5$).

2.7.2 Quantitative validation

In our experiments, we assumed that a calibration curve and its corresponding QCs were accepted if 6 out of 8 CS concentration levels and, at least 4 out of 5 QC samples for each QC level (= 80% of the QCs samples, corresponding to the β-expectation tolerance interval described by the SFSTP [42–44]) satisfied the validation criteria. This approach is a derivation of EMA guidelines, which recommend that 67% of QC samples for 50% QC level must fulfill the bias acceptance criteria.

For the validation of the quantitative method, the calibration curve was fitted by least square regression using 8 CS concentration levels, ranging from 0.40 µg/mL to 200 µg/mL, and different weighting factors were evaluated (1, 1/concentration, 1/concentration^2). Linearity was assessed from the slope of the linear regression and the y-intercept and the coefficient of determination (R^2). For the validation of the method, accuracy, precision, and recovery were tested with the same QC sample. Accuracy, repeatability, and intermediate precision were assessed using five determinations with independents extractions of the same batch, on three separate days (n = 15) for each of the six QC levels using human plasma, and each of the three QC levels using murine plasma loaded with paraoxon. Accuracy was calculated by the mean bias between the observed back-calculated concentration ($C_{measured}$) and the theoretical concentration ($C_{theoretical}$), i.e. $Bias(\%)=100\times(C_{measured}-C_{theoretical})/C_{theoretical}$. Within-assay accuracy was calculated for each day using the 5 available values, and within-assay precision was determined for each QC level from its mean back-calculated concentration and mean variance (i.e. coefficient of variation(%)=100×standard deviation/mean value). Cochran test (alpha = 0.05) was used to check homogeneity of variances over the 3 days before using the mean variance. Between-assay precision and accuracy were calculated for the 6 QC levels on 3 values (i.e. one value per day). For each day, the selected value was the one presenting the most important bias. For each QC level, between-days precision and accuracy were respectively the coefficient of variation and the mean bias calculated on these three selected samples respectively. Both precision and accuracy were combined as the tolerance interval to build the accuracy profile. The lower limit of quantification (LLOQ) and the upper limit of quantification (ULOQ) of the method were both set to the lowest and the highest QC value (0.40 µg/mL and 150 µg/mL), which is another adaptation of EMA guidelines. Mean relative errors (%) from the expected concentrations were calculated and the accepted ranges were ± 20 % and ± 15 % for the lowest QC concentration (i.e. 0.40 µg/mL), and the other QC, respectively. Acceptance criteria limits for the β-expectation tolerance interval were 100 ± 20% for the first QC level (LLOQ), and 100 ± 15% for other QC levels. The carryover was also investigated with the injection of the highest calibration standard (200 µg/mL), followed by five injections of blank plasma extract. Carryover was considered negligible if the signal obtained with the 1st blank following the highest standard was less than 20% of the LLOQ.

2.7.3 Extraction recovery and stability

Two calibration curves were carried out, the difference was in the moment of the (*R*)-CE3F4 addition. The first calibration curve corresponded to addition into plasma before the extraction process (calibration "A"), and the second calibration curve consisted in the addition of the (*R*)-CE3F4 after the extraction process on blank plasma with ACN, and it corresponds to a theoretical recovery of 100 % (calibration "B") [45]. Samples were injected into the chromatographic system. The recovery was calculated each day of the validation process with the ratio between the slopes of these 2 calibration curves (A/B).

The stability of the extracts in the autosampler (set at 20° C) was investigated over a 15 h period by comparing the concentration obtained with extracts divided into two batches. One was injected immediately after extraction then reinjected after 15 h in the autosampler, and the other batch was just injected once after 15 h in the autosampler. The stability over one year was investigated for stock solutions for their usual storage conditions (5° C), one month for human QCs or one week for mouse QCs stored at -20° C, after 3 cycles of freeze-thaw (-20° C to ambient temperature), and short-term stability for two hours at room temperature. If a decrease of 15 % or more was observed for QC or 5 % for stock solutions, the analyte was considered unstable for the corresponding tested condition.

2.8 Evaluation of (R)-CE3F4 ex vivo stability in human or murine plasma

2.8.1 (R)-CE3F4 behaviour in plasma at 37°C

The stability of (*R*)-CE3F4 in human and murine plasmas was investigated ex vivo for 24 hours at 37°C. Due to the poor solubility in water media, (*R*)-CE3F4 was first solubilized into DMSO to obtain a stock solution at 10 mg/mL. 3.6 µL of the (*R*)-CE3F4 solution was mixed to 600 µL plasma in microcentrifuge tubes to obtain a concentration near 60 µg/mL. Microcentrifuge tubes were put in a rotary agitator at 37°C. Sampling was achieved at the following times (t = 5', 15', 30', 45', 60', 90', 120', 180', 20 h and 24 h). To follow the stability of the (*R*)-CE3F4 over time, a normalization of the data was made by the ratio between the concentration measured at each sampling time and the concentration measured at 5 minutes ($[CE3F4]_t/[CE3F4]_{5min}$ = relative concentration (%) at time *t*). Experiments were repeated four times with human plasma, and six times with murine plasma.

2.8.2 Stabilization studies of (R)-CE3F4 in murine plasma at 37°C with EDTA, paraoxon, BNPP, or benzil

Paraoxon, BNPP, benzil, and EDTA were separately tested as metabolism inhibitors in murine plasma to stop the degradation of (*R*)-CE3F4 that may occur during the processing of

samples *in vivo* studies. EDTA was tested at the concentration of 10 mM in murine plasma sample (i.e. 15 µL of the EDTA stock solution were added to 284 µL of plasma) spiked with (*R*)-CE3F4 (i.e. 1.8 µL of (*R*)-CE3F4 at 10 mg/mL for 300 µL of plasma) and the sample was put in a rotary agitator at 37°C after one-minute vortex step. Paraoxon, BNPP, and benzil were studied separately at 10^{-4} M, 10^{-5} M, 10^{-6} M in plasma. Briefly, for these three inhibitors, 3.0 µL of each stock solution (at 10^{-2} M, 10^{-3} M, 10^{-4} M) were added in 296 µL of murine plasma, followed by a one-minute vortex step and five minutes in a rotary agitator at 37°C. Then, (*R*)-CE3F4 was added in plasma already loaded with inhibitor (paraoxon or BNPP or benzil) in the same proportions described in the paragraph above (i.e. 1.8 µL of (*R*)-CE3F4 at 10 mg/mL for 300 µL of plasma). For the four compounds, five sampling times were analysed for up to 1 hour to estimate the stabilization of the (*R*)-CE3F4 in samples. Similarly, in a second experiment (*R*)-CE3F4 and paraoxon (stock solution at 10^{-2} M) were simultaneously added in murine plasma at the same proportion and conditions of the previous experiment to evaluate whether (*R*)-CE3F4 degradation occurred during homogenization of the sample.

2.8.3 Storage conditions suitable for (R)-CE3F4 in murine plasma

The stability of loaded murine plasma samples with paraoxon (10^{-4} M in plasma sample) and (*R*)-CE3F4 (60 µg/mL) was investigated at 5° C for 3 days, after 3 days and one week at -20° C, and after 3 cycles of freeze-thaw. If a decrease of 15% or more was observed, samples were considered unstable.

2.8.4 HPLC-MS/MS for metabolite identification

The identification of (*R*)-CE3F4 metabolite was performed by HPLC-MS/MS analysis. To proceed with the identification, a control sample of (*R*)-CE3F4 (5 µg/mL), a control sample of deformylated-CE3F4 (5 µg/mL), and plasma extract (as described in 2.8.1) were analyzed.

2.9 Evaluation of (R)-CE3F4 protection against enzymatic degradation by various formulations

Three different formulations were used first to solubilize the (*R*)-CE3F4 to obtain a final concentration of 625 µg/mL. In the case of DSPE-PEG_{2000} micelles, a thin-film hydration method was used [46]. Briefly, (*R*)-CE3F4 was incorporated simultaneously with DSPE-PEG_{2000} in the chloroform solution, then the mixture was dried at ambient temperature for 60 min using a rotary evaporator R-215 (Büchi, Switzerland) and the obtained film was hydrated with PBS at room temperature ([DSPE-PEG_{2000}] = 25 mM, $[(R)\text{-CE3F4}]_{\text{post process}}$ = 900 µg/mL). In the cas of Solutol/PEG, a mixture of Solutol HS 15, PEG_{200}, and PBS (4.5:1:15,

$m_{PEG200}/m_{Solutol\ HS\ 15}/v_{PBS}$) was used. For 1.0 mL of preparation, 0.625 mg of (*R*)-CE3F4 was dissolved in 225 mg of PEG_{200} at 40°C, then 50 mg of Solutol HS 15 was added (4.5:1:15, $m_{PEG200}/m_{Solutol\ HS\ 15}/v_{PBS}$), and the mixture was gently homogenized for 30 min at 40°C. After this step, 750 µL of PBS at 40°C was added and the formula was gently mixed 10 min at 40°C then 1h at room temperature ($[(R)\text{-CE3F4}]_{post\ process}$ = 625 µg/mL). In the case of lipid nanocapsules (LNC), a phase inversion process was used [47]. PBS was used as an aqueous phase, and a mixture of Solutol HS 15, EggPC, and Miglyol® as lipid phase. For 5 mg of (*R*)-CE3F4, the lipids proportions were 57.8% Mygliol, 37.0% Solutol HS 15 and 5.2% EggPC for a total amount of lipids of 2590 mg, and 1.1 mL of PBS. (*R*)-CE3F4 was first dissolved into Miglyol before the process. Both phases were mixed into a vial containing a magnet. The vial was put into a water bath, and three temperature cycles of heating/cooling between 55°C and 85 °C were applied. After reaching 85°C for the third time, the vial was cooled to 75°C and a dilution with 3 mL of cold PBS (5°C) was performed under magnetic stirring, leading to the spontaneous formation of lipid nanocapsules ($[(R)\text{-CE3F4}]_{post\ process}$ = 900 µg/mL).
All three formulations were centrifuged at 4,000 g for 10 min to remove non-solubilized (*R*)-CE3F4. Supernatants were collected, (*R*)-CE3F4 concentration was measured and adjusted with PBS to obtain a final concentration of 625 µg/mL. The analytical method was applied to monitor the (*R*)-CE3F4 concentration in C57BL/6 plasma samples at 37°C.

3 Results and discussion

3.1 Spectral analysis of (R)-CE3F4 & method validation

3.1.1 Spectral analysis

Due to the lack of information on (*R*)-CE3F4, a preliminary study of the UV absorption spectra was performed in the range of 200 nm to 400 nm. This enables us to determine precisely the suitable wavelengths for HPLC-UV analysis. From the mean UV spectrum of (*R*)-CE3F4, two narrow bands, showing maxima at 202 nm and 220 nm, and two broad bands were observed (**Fig. S1**). The second derivative spectrum was calculated from the mean UV spectrum to exalt the spectrum signal and the two expected wavelengths from the broad bands were highlighted at 250 and 299 nm. Based on the variability of the measured absorbances (RSD %) at 202 nm, 220 nm, 250 nm, and 299 nm, which were 6.1 %, 2.12 %, 3.0 %, and 10.4% respectively, we selected the wavelengths 220 nm and 250 nm for the quantification of (*R*)-CE3F4. Then both wavelengths were further investigated to improve the UV detection for

the quantitative method depending on the specificity of the chromatographic assay on human and murine plasma.

3.1.2 Validation of the (R)-CE3F4 method quantification in human plasma

The next step for conducting the CE3F4 bioanalysis was to set up a quantitative method using liquid chromatography. The relative hydrophobicity of CE3F4 (LogP= 3.6) allowed us to use a reversed stationary phase with a long alkyl chain (C18) and relative eluotropic strength (ACN/Water: 60/40 (v/v)). Accordingly, the method was validated in terms of specificity, linearity, LOQ, accuracy profile, and precision. Carryover, sample stability, and extraction recovery were also determined.

Under these analytical conditions, the (*R*)-CE3F4 had an elution time of 4.2 min and was well-separated from visible compounds from the human plasma matrix which were overwhelmingly eluted up to 3 min. Indeed, concerning the specificity, no signal was detectable at 220 or 250 nm on the 6 different blank human plasma samples close to CE3F4 retention time (4.2 min) as displayed in **Fig. 2**. Similar results were obtained with enzyme inhibitors, or commonly used compounds for *in vivo* studies as isoflurane, Rompun® (xylazine), or the association of Zoletil® (tiletamine, zolazepam) at a lethal dose, or excipients for the formulation of the (*R*)-CE3F4 (PEG_{200}, Solutol HS 15, EggPC, DSPE-PEG_{2000}, Miglyol 812). At this stage, it is worth noting that two calibration curves corresponding to each selected wavelength (i.e. 220 and 250 nm) were performed. This strategy was applied to overcome the difference between species, with the possible interferences generated by matrix elements extracted from human or mouse plasma.

For the validation of the (*R*)-CE3F4 method quantification in human plasma, the β-expectation proportion of 80% for all QC level, using tolerance interval calculation, was more appropriate than that recommended by bioanalytical methods (67% of validated QC for at least 50% of QC levels fulfilling acceptance criteria). For QC, the validation domain ranged from 0.40 to 150 µg/mL to cover the concentration range observed in the only *in vivo* study on CE3F4 [2]. However, these authors did not measure the concentration of CE3F4 in blood or plasma. An amount of 3 mg/kg was injected into C57BL/6 mice for an average total blood volume estimated to 72 mL/kg [48]. Therefore, the maximum blood concentration of CE3F4 that could be observed should be 42 µg/mL assuming a one-compartment model for blood (plasma + cells). However, if CE3F4 is only located in plasma (where the plasma volume is around 36-43 mL/kg for a usual hematocrit ranging from 40 to 50% [49]), the expected

maximum concentration should reach at least 83 µg/mL for a dosage of 3 mg/kg. Consequently, a calibration curve covering concentrations from 0.40 to 150 µg/mL was considered appropriate to evaluate the maximal concentration to 1% of the maximal expected concentration for the dosage of 3 mg/kg. In addition, such a calibration curve allows plasma quantification in plasma with the same sample treatment procedure for variable dosage regimens (i.e. no dilution step). These extended ranges led us to assess calibration curves from 0.40 to 200 µg/mL with various weighted regressions including no weighing, 1/concentration, and 1/concentration². The calibration curves were obtained without using internal standard since no appropriate CE3F4 analog was commercially available. Although each calibration curve provided an acceptable coefficient of determination R^2 (> 0.99), only 1/concentration² weighting fulfilled the relative error acceptance range for all levels (i.e. within ± 20% for the lowest concentration, ± 15% for other levels). The parameters of the calibration curves at 220 and 250 nm were determined (**Table 3**) and they satisfied the validation criteria, including their corresponding QCs (**Table 4**). Within-day and between-days accuracies and precisions were satisfactory.

Accuracy profiles were built from data combining precision and trueness (**Fig. S2**). At 220 nm, biases were shown into the interval of ± 10 %, and RSD < 10 % for LLOQ and < 5 % for other QCs. These values satisfied EMA criteria for the validation of bioanalytical methods. Based on these evaluated parameters, the corresponding accuracy profile at 220 nm has been built (**Fig. S2A**). The tolerance interval was between the limits given by the EMA (100 ± 20% for LLOQ, and 100 ± 15% for another QC level) for a β-expectation tolerance interval set at 80%. These results allowed concluding that the method fulfilled the required reliability in terms of trueness and precision for the quantification of (*R*)-CE3F4 in the plasma matrix. The LLOQ and ULOQ were very satisfactory with values of 0.40 µg/mL and 150 µg/mL, respectively. For the calibration curve at 250 nm, very similar results about biases and RSD were obtained (biases are into the interval of ± 10%, and RSD <10%). The corresponding accuracy profile is reported in **Fig. S2B**, where it appears that the tolerance interval for LLOQ was near the upper acceptance limit but was still conforming (119.8%). Finally, the calibration curves for human plasma at the two wavelengths satisfied the EMA criteria. Also, the method demonstrated a strong ability to accurately quantify (*R*)-CE3F4, even considering the tolerance interval for each QC level. For the carryover, the signal was less than 20% of the

LLOQ on the first injection of blank plasma at the retention time of the analyte (no peak detectable) after the injection of the highest concentration used for calibration (200 µg/mL). Besides, the extraction of CE3F4 was assessed from calibration curve "A" (i.e. CE3F4 addition into plasma before the extraction process) and calibration curve "B" as reference (i.e. CE3F4 addition after extraction process on blank plasma). The simple extraction procedure, which consisted to precipitate proteins with 150 µL of ACN, followed by a centrifugation step, allowed a mean extraction recovery on three days of 100.4% with an RSD of 6.4%. Consequently, the use of an internal standard was unnecessary due to a total extraction, a low RSD, and UV detection, contrarily to mass spectrometry, which involves an ionization yield in the case of a coelution with molecules from the complex matrix, justifying the use of an internal standard to reduce variability and correct bias (i.e. isotope-labeled CE3F4).

3.1.3 Human plasma samples stability

The stability of the extracted samples was investigated from the validated calibration curve. After 15 h in an autosampler, the bias between the first and second analysis session was superior to 15 % for samples that were first injected due to solvent evaporation, but the stability was correct for non-immediately injected samples (less than 15% loss). Concerning stock solutions stored at 5°C for one year, QCs stored at -20°C for one month, or exposed to 3 cycles of freeze-thaw, or after two hours at room temperature, degradation was not significant (< 5% for stock solutions, < 15% for all conditions using plasma). It can be concluded that such results make it possible to obtain sufficient stability to organize analyses by a campaign, at a still experimental stage of pharmaceutical development. More long-term stability could be explored if the (*R*)-CE3F4 exhibits a clinical interest to be tested in humans.

3.2 Application of the LC-UV method to the evaluation of (R)-CE3F4 ex vivo stability in human or murine plasma

Various risk points were verified to check the transposability of the HPLC-UV method, in particular concerning the specificity of the signal, and the extraction efficiency of CE3F4.

3.2.1 Chromatograph difference in specificity between human and murine plasma

As previously mentioned, the results on specificity showed no detectable signal near CE3F4 at 220 or 250 nm on blank human plasma samples, but differences resulted with blank murine plasma samples. Indeed, visible peaks at the CE3F4 retention time (4.2 min) were observed in these matrices at 220 nm (**Fig. 3A**). When switching to 250 nm, detection specificity was

enhanced and thus satisfactory, without any visible coelution impacting CE3F4 quantification (**Fig. 3B**). Different gradient conditions were studied (results not shown), but none of them adequately improved the resolution at 220 nm in addition to extending the time analysis (until one hour). These results are in agreement with our previous hypothesis on the interest to validate several detection conditions when UV detection is used (i.e. 220 and 250 nm) because of the possible interferences on chromatograms depending on the origin of the plasma (i.e. mouse or human). Therefore, the wavelength of 250 nm should be used for quantification in mouse plasma, and both 220 and 250 nm are suitable for human plasma analysis.

3.2.2 (R)-CE3F4 and ex vivo plasmatic metabolism at 37°C

We first investigated *ex vivo* the (*R*)-CE3F4 behavior in the plasmas from two species as a function of the time to evaluate a potential plasma metabolism at 37°C. To be suitable for HPLC analysis, samples were treated as described previously, and chromatograms were collected using wavelengths 220 and 250 nm for human and mouse plasma, respectively. The chromatographic analysis of the murine and human plasma samples showed a peak at 8.6 min (TRR = 2.05) at 220 nm and 250 nm (**Fig. 4**) in addition to CE3F4 (4.2 min). Also, a lack of specificity was observed at 220 nm at 4.2 min in murine plasma (**Fig. 4A**), by using the appropriate wavelength detection at 250 nm, the peak was recovered, confirming the usefulness of this wavelength for preclinical studies in mice.

A significant difference in the kinetics of the disappearance of the main peak was observed between the two plasma samples. Indeed, a decrease of 23 % of the peak area was observed in human plasma after 24 h (**Fig. 5A**). In contrast, a decrease of 95 % was found in murine plasma after only 3 h, and no peak at the expected time was detected after six hours confirming the total degradation of CE3F4 (**Fig. 5A**). These results suggest that (*R*)-CE3F4 undergoes distinct kinetic degradation. The observed half-life in murine plasma was 39.9 min (confidence interval 95%: from 36.9 to 43.4 min) against a half-life superior to 24 h in human plasma. As depicted in **Fig. 5B**, the CE3F4 related metabolite showed two phases in murine plasma, an acute ascending phase, and a slow decreasing phase suggesting the instability of the metabolite in murine plasma (e.g. due to the formation of secondary metabolites, or non-enzymatic degradation such as oxidation reaction). For human plasma, this metabolite appeared very slowly.

We therefore hypothesized that enzyme-dependent hydrolysis promoted metabolism on the (*R*)-CE3F4 N-formyl group (**Fig. S3**) resulting in a more apolar compound than (*R*)-CE3F4 which is coherent with the HPLC analysis exhibiting a longer elution time than (*R*)-CE3F4 on the reverse-phase column. The spectral analysis of this degraded CE3F4 showed similar features with the original CE3F4 spectrum depicting three maxima (218 nm, 250 nm, and 325 nm), indicating a structural similarity with the CE3F4 (**Fig. S4**). Among the known CE3F4 derivatives, deformylated-CE3F4 may be a candidate. To confirm this structural hypothesis, LC-UV and LC-MS/MS analyses were performed on synthesized deformylated-CE3F4 as described in a specific part below (3.3). It is worth mentioning that the deformylated-CE3F4 was inactive on EPAC1 [3]. On this metabolism through N-deformylation, Gleason et *al.* reported an inter-species variability on the plasmatic metabolism of diformyldapsone. Different kinetics of metabolism have been described in plasmas, in the following order: mouse > rat > guinea pig > rabbit, while no N-deformylation in the dog or human plasma was observed [19]. Some authors observed differences in plasma metabolism between rodents, dogs, and humans for an N-formylated indolocarbazole topoisomerase I inhibitor [20], with no N-deformylation in dogs or humans plasma. Other studies also reported similar differences between species in the type of plasmatic esterases [23,38,39,50]. They noticed the absence of carboxylesterases in human plasma in contrast to rodent plasmas. However, liver metabolism showed an inversed tendency for humans and rodents. Another study on diformyldapsone with liver homogenates changed the rank order of metabolism rates: guinea pig ≥ human > mouse = rabbit = rat > dog [18]. Based on these results, it appears evident to consider enzyme inhibitors to stabilize samples following plasma collection, for *in vivo* kinetic experiments, especially in mice.

3.2.3 Stabilization studies of (R)-CE3F4 in murine plasma at 37°C with paraoxon

To proceed to the (*R*)-CE3F4 quantification in murine plasma, different strategies were explored using either EDTA, paraoxon, BNPP, or benzil. EDTA can inhibit metal-dependent enzymes, such as hydrolases including e.g. amidohydrolase [51] or paraoxonase [23,52,53] in addition to being of interest as an anticoagulant for sample collection. Paraoxon is known as a well-known powerful esterase inhibitor (organophosphate oxon), as described by Gleason and *al*. [19] for diformyldapsone stabilization in plasma samples. BNPP and benzil are more specific inhibitors than paraoxon. BNPP is a specific inhibitor of carboxylesterases [54,55],

phosphodiesterase [56]. Benzil is a specific reversible inhibitor of mammalian carboxylesterases [57].

EDTA did not exhibit any stabilizing effect against CE3F4 degradation in murine plasma samples. Thus, the enzyme involved in CE3F4 degradation is not metal-dependent. Nevertheless, it could be interesting to note that EDTA can inhibit the paraoxonase at 5 mM [23] and be used in this study at 10 mM. The enzyme is involved in the metabolism of organophosphate like paraoxon.

Paraoxon was tested at different concentrations to stop the degradation of CE3F4. It has been shown that plasmatic N-deformylation was inhibited with paraoxon. Firstly, paraoxon was added in the plasma 5 min before the (*R*)-CE3F4 for homogenization of the sample to allow at least a 1-hour blockade. This 1-hour delay was chosen to mimic conditions of sample treatment (i.e. blood sampling, centrifugation step for plasma/serum separation, until protein precipitation by solvents). The inhibition of CE3F4 degradation was null, partial, and total for paraoxon at 10^{-6} M, 10^{-5} M, and 10^{-4} M, respectively (**Fig. 6**). These results confirmed the relevance of paraoxon to inhibit plasmatic deformylation of CE3F4 and subsequently, the stabilization of plasma samples. Moreover, the paraoxon experiments suggest the involvement of a hydrolase in CE3F4 metabolism. Secondly, when 10^{-4} M paraoxon was added simultaneously with (*R*)-CE3F4 to mimic real sample treatment (i.e. addition of paraoxon as first pre-treatment step after blood sampling), no CE3F4 degradation was observed and no metabolite was detected on the chromatograms (data not shown).

BNPP and benzil were assayed, but they did not stabilize the CE3F4 against degradation on a 1-hour duration (**Table 5**). A slight concentration-dependent inhibition was observed with BNPP, but it appears that higher concentrations should be considered to obtain sufficient inhibition, which is of no interest in practice. These results exhibit that carboxylesterases are not involved in CE3F4 degradation. Consequently, the paraoxon at the inhibiting concentration of 10^{-4} M was retained to allow mouse sample pre-treatment.

3.2.4 Validation of the (R)-CE3F4 method quantification in murine plasma loaded with paraoxon

Based on the validation procedure in human plasma, and the stabilization of CE3F4 in murine plasma thanks to paraoxon, the validation of the (R)-CE3F4 quantification method at 250 nm in murine plasma loaded with paraoxon has been carried out. As for validation in human plasma, only 1/concentration² weighting fulfilled the relative error acceptance range for all

levels (i.e. within ± 20% for the lowest concentration, ± 15% for other levels). The parameters of the calibration curves at 250 nm were determined (**Table 6**) and shown to satisfy the validation criteria.

As observed in human plasma, no carryover was observed on the first injection of blank murine plasma at the retention time of the CE3F4 (no peak detectable) after the injection of the highest concentration used for calibration (200 µg/mL), and the mean extraction recovery on three days was 100.5% with an RSD of 2.3%. Then paraoxon did not influence the CE3F4 extraction in murine plasma. Because of similarities of results between human plasma and murine plasma loaded with paraoxon, three QC levels were used to rationalize the use of animals for the transposition of the already fully validated method in human plasma. The results on QCs were satisfactory (**Table 7**) because all biases were shown in the interval of ± 5%, and RSD < 5%. The corresponding accuracy profile is reported in **Fig. S7**.

Thus, the validated method using human plasma allowed to manage murine samples, and then the method was validated on three days in murine plasma loaded with paraoxon allowing the quantification of CE3F4 at 250 nm from 0.40 to 150 µg/mL.

3.2.5 Murine sample storage

For the stability of murine plasma spiked with paraoxon 10^{-4} M, a critical degradation of the (*R*)-CE3F4 was observed after three days at 5°C (-79.6%). However, no significant variations (< 15%) were observed at -20°C after 1 week, after 3 cycles of freeze-thaw, after two hours at room temperature, or in the plasma extracts after 15h in the autosampler. This could be explained by the presence of paraoxonase in murine plasma, which degrades paraoxon and then allows the hydrolysis of CE3F4. This hypothesis could be surprising because paraoxon is known as an irreversible inhibitor. However, a spontaneous reactivation of mouse butyrylcholinesterase after paraoxon inhibition has been described by Li et al. [23], and pieces of evidence of other inhibition mechanisms such as the allosteric modification or steric hindrance which can be reversible were reported [58–60].

Thus, storage at -20°C facilitates the practical aspect of handling biological samples, allowing flexibility in analysis schedules. Storage at -80°C should be considered and evaluated for the long-term storage of biological samples.

3.3 Identity of the main metabolite

3.3.1 HPLC-UV analysis

In addition to the efficacy of paraoxon in inhibiting the degradation of CE3F4 in murine plasma, similarities were observed between unknown metabolites and deformylated-CE3F4. Samples were prepared to obtain relatively close concentration (i.e. deformylated-CE3F4 and (*R*)-CE3F4 at 50 µg/mL in ACN versus 100 µg/mL of (*R*)-CE3F4 in murine plasma analysed after a little more than a half-life). The RP-LC analysis resulted in similar relative retention times: 2.05 and 2.08 for deformylated-CE3F4 and observed metabolite, respectively (**Fig. S5A**). A small peak corresponding to a synthesis impurity of (*R*)-CE3F4 was detected at 5.2 min. When analysing the UV spectra of deformylated-CE3F4 and metabolite, the high similarity was obtained with three identical maxima at 218 nm, 250 nm, and 322 nm (**Fig. S5B**). These results supported the hypothesis that the metabolite observed in murine plasma was the deformylated-CE3F4.

3.3.2 HPLC-MS/MS analysis

To undoubtedly confirm the structure of CE3F4 metabolite as deformylated-CE3F4 and so the mechanism involved in CE3F4 degradation, mass spectrometry (MS) experiments were performed. Deformylated-CE3F4 presents a molar mass of 322.9 g/mol which corresponds to a parent ion of m/z of 323.9 in positive mode [MH^+]. Total ion chromatograms (TIC) and extracted chromatograms (m/z 323.9, m/z 351.9) of plasma sample, deformylated-CE3F4 and (*R*)-CE3F4 controls are presented in **Fig. 7**. It should be noted that because the flow rate of the mobile phase is 0.5 mL/min instead of 1.0 mL/min in previous experiments, the time of retention of analytes was doubled. Indeed, (*R*)-CE3F4 is eluted at 8.4 minutes, whereas the unknown metabolite is eluted at 18.3 minutes. The unknown metabolite and deformylated-CE3F4 are eluted with the same retention time. Regarding MS experiments, the hypothesized metabolite and deformylated-CE3F4 exhibited the same parent ion of m/z 323.9 as observed on the chromatogram of the extracted ion m/s 323.9 (**Fig. 7A & C**) and the comparison of the MS spectrum extracted at 18.3 min of plasma sample (**Fig. 8A**) and deformylated-CE3F4 (**Fig. 8B**). Also, the isotopic distribution is similar and is coherent with the presence of two bromine (**Fig. 8C & D**). Finally, both the unknown metabolite and deformylated-CE3F4 showed the same MS fragmentation pattern of the parent ion (**Fig. 8E & F**). Altogether, these results confirmed that the metabolite observed in murine plasma was the deformylated-CE3F4. MS and MS/MS spectrum of CE3F4 were also recorded and are presented in supplemental data (**Fig. S6**).

3.4 Application to the evaluation of (R)-CE3F4 protection against enzymatic degradation by various formulations.

For all formulations, the degradation of (*R*)-CE3F4 in plasma followed an exponential decay (R^2 >0.99), allowing the estimation of an apparent half-life linked to the ability of the formulation to protect the (*R*)-CE3F4 against enzymatic degradation. As synthetized in **Table 8**, the formulations exhibited different protection levels. When solubilized in micelles, the (*R*)-CE3F4 degradation was equivalent to (*R*)-CE3F4 solubilized in DMSO (apparent half-life of 0.8 h), indicating a lack of protection of the (*R*)-CE3F4 by this formulation. The Solutol HS 15/PEG_{200} mixture showed an intermediate level of protection, with a (*R*)-CE3F4 apparent half-life of 2.7 h. Lipid nanocapsules provided the most important protection effect with an apparent half-life of 5.5 h for (*R*)-CE3F4. Thus, the analytical method described in this study proved efficient for the identification of promising formulations able to optimize (*R*)-CE3F4 administration for future pharmaceutical development.

4 Conclusion

The quantification method including a simple extraction protocol showed to be well suitable for the quantification of the (*R*)-CE3F4 in plasma for preclinical studies as well as clinical studies. This method allows drug quantification in complex matrices from different origins providing that appropriate wavelength selection is performed. Because of the impact of the matrix observed at 220 nm in murine plasma that is still unresolved despite the application of different gradient conditions, an adaptation of the wavelength in agreement to the studied species was necessary (220 nm or 250 nm for human samples, only 250 nm for mouse samples) highlighting the importance of the wavelength selection for the (*R*)-CE3F4 quantification.

The validated method allows the processing of the samples and the rendering of the results within the same working day. Moreover, it permits to follow the main metabolite of (*R*)-CE3F4 observed in mouse plasma within the same analysis. The metabolite was identified as the N-deformylated-CE3F4 and the involvement of a hydrolase was revealed by paraoxon use and further by HPLC-UV and HPLC-MS/MS studies.

We also show the interest of paraoxon in preclinical studies to stop metabolic degradation during sample pretreatment in mouse models. Future studies are needed to identify the enzyme responsible for the observed degradation, for the possible development of knock-out mice models lacking this enzyme [61] for pharmacokinetic and efficacy studies.

Furthermore, non-plasma-based metabolic pathways should be considered, like metabolic stability assay on microsomes or hepatocytes knowing that hepatic metabolism is central in humans, to elucidate the (*R*)-CE3F4's metabolic profile and then identify any novel metabolites and metabolic pathways in humans and mice. To conclude in an objective of pharmaceutical development, it appears essential to provide for the protection of the (*R*)-CE3F4 against all potential enzymatic degradations (i.e. also in the liver for humans), and to develop an appropriate formulation accordingly.

Acknowledgment

The "Institut Galien Paris-Sud" and the "Service de Chimie Bioorganique et de Marquage" belong to the Laboratory of Excellence in Research on Medication and Innovative Therapeutics (ANR-10-LABX-0033-LERMIT).

Conflict of Interest

The authors declare no conflict of interest regarding this publication.

References

[1] B. Ziaeian, G.C. Fonarow, Epidemiology and aetiology of heart failure, Nat Rev Cardiol. 13 (2016) 368–378. https://doi.org/10.1038/nrcardio.2016.25.

[2] R. Prajapati, T. Fujita, K. Suita, T. Nakamura, W. Cai, Y. Hidaka, M. Umemura, U. Yokoyama, B.C. Knollmann, S. Okumura, Y. Ishikawa, Usefulness of Exchanged Protein Directly Activated by cAMP (Epac)1-Inhibiting Therapy for Prevention of Atrial and Ventricular Arrhythmias in Mice, Circulation Journal. 83 (2019) 295–303. https://doi.org/10.1253/circj.CJ-18-0743.

[3] D. Courilleau, M. Bisserier, J.-C. Jullian, A. Lucas, P. Bouyssou, R. Fischmeister, J.-P. Blondeau, F. Lezoualc'h, Identification of a tetrahydroquinoline analog as a pharmacological inhibitor of the cAMP-binding protein Epac, J. Biol. Chem. 287 (2012) 44192–44202.

[4] D. Courilleau, P. Bouyssou, R. Fischmeister, F. Lezoualc'h, J.-P. Blondeau, The (R)-enantiomer of CE3F4 is a preferential inhibitor of human exchange protein directly activated by cyclic AMP isoform 1 (Epac1), Biochem. Biophys. Res. Commun. 440 (2013) 443–448.

[5] M. Metrich, M. Berthouze, E. Morel, B. Crozatier, A.M. Gomez, F. Lezoualc'h, Role of the cAMP-binding protein Epac in cardiovascular physiology and pathophysiology, Pflugers Arch. 459 (2010) 535–546.

[6] S.S. Hothi, I.S. Gurung, J.C. Heathcote, Y. Zhang, S.W. Booth, J.N. Skepper, A.A. Grace, C.L.-H. Huang, Epac activation, altered calcium homeostasis and ventricular arrhythmogenesis in the murine heart, Pflugers Arch - Eur J Physiol. 457 (2008) 253–270. https://doi.org/10.1007/s00424-008-0508-3.

[7] A.-C. Laurent, M. Bisserier, A. Lucas, F. Tortosa, M. Roumieux, A. De Régibus, A. Swiader, Y. Sainte-Marie, C. Heymes, C. Vindis, F. Lezoualc'h, Exchange protein

directly activated by cAMP 1 promotes autophagy during cardiomyocyte hypertrophy, Cardiovasc. Res. 105 (2015) 55–64.
[8] M. Bisserier, J.-P. Blondeau, F. Lezoualc'h, Epac proteins: specific ligands and role in cardiac remodelling, Biochemical Society Transactions. 42 (2014) 257–264. https://doi.org/10.1042/BST20140033.
[9] M. Zhang, J. Zheng, W. Wang, F. Kong, X. Wu, J. Jiang, J. Pan, Exchange-protein activated by cAMP (EPAC) regulates L-type calcium channel in atrial fibrillation of heart failure model, Eur Rev Med Pharmacol Sci. 23 (2019) 2200–2207.
[10] R. Lorenz, T. Aleksic, M. Wagner, G. Adler, C. Weber, The cAMP/Epac1/Rap1 Pathway in Pancreatic Carcinoma, Pancreas. 37 (2008) 102–103. https://doi.org/10.1097/MPA.0b013e318160748f.
[11] N. Kumar, S. Gupta, S. Dabral, S. Singh, S. Sehrawat, Role of exchange protein directly activated by cAMP (EPAC1) in breast cancer cell migration and apoptosis, Mol Cell Biochem. 430 (2017) 115–125. https://doi.org/10.1007/s11010-017-2959-3.
[12] D.-P. Sun, C.-L. Fang, H.-K. Chen, K.-S. Wen, Y.-C. Hseu, S.-T. Hung, Y.-H. Uen, K.-Y. Lin, EPAC1 overexpression is a prognostic marker and its inhibition shows promising therapeutic potential for gastric cancer, Oncology Reports. 37 (2017) 1953–1960. https://doi.org/10.3892/or.2017.5442.
[13] I. McPhee, L.C.D. Gibson, J. Kewney, C. Darroch, P.A. Stevens, D. Spinks, A. Cooreman, S.J. MacKenzie, Cyclic nucleotide signalling: a molecular approach to drug discovery for Alzheimer's disease, Biochemical Society Transactions. 33 (2005) 3.
[14] C.M. Middeldorp, J.M. Vink, J.M. Hettema, E.J.C. de Geus, K.S. Kendler, G. Willemsen, M.C. Neale, D.I. Boomsma, X. Chen, An association between Epac-1 gene variants and anxiety and depression in two independent samples, Am. J. Med. Genet. 153B (2010) 214–219. https://doi.org/10.1002/ajmg.b.30976.
[15] M4S Common Technical Document for the Registration of Pharmaceuticals for Human Use - Safety, Committee for Human Medicinal Products. (2003) 113.
[16] M4E(R2) - Common technical document for the registration of pharmaceuticals for human use - Efficacy, Committee for Human Medicinal Products. (2016) 53.
[17] T. Tuntland, B. Ethell, T. Kosaka, F. Blasco, R.X. Zang, M. Jain, T. Gould, K. Hoffmaster, Implementation of pharmacokinetic and pharmacodynamic strategies in early research phases of drug discovery and development at Novartis Institute of Biomedical Research, Frontiers in Pharmacology. 5 (2014).
[18] C.Y. Chiou, Deformylation of 4,4'-diformamidodiphenyl sulfone (DFD) by mammalian liver homogenates, Biochemical Pharmacology. 20 (1971) 2401–2408. https://doi.org/10.1016/0006-2952(71)90240-1.
[19] L.N. Gleason, B.P. Vogh, Deformylation of 4,4'-diformamidodiphenyl sulfone (DFD) by plasma of certain mammals, Biochemical Pharmacology. 20 (1971) 2409–2416. https://doi.org/10.1016/0006-2952(71)90241-3.
[20] N. Takenaga, T. Hasegawa, M. Ishii, H. Ishizaki, S. Hata, T. Kamei, In vitro metabolism of a new anticancer agent, 6-N-formylamino-12,13-dihydro-1,11-dihydroxy-13-(β-D-glucopyranosil)5H-indolo [2,3-A]pyrrolo [3,4-C]carbazole-5,7(6H)-dione (NB-506), in mice, rats, dogs, and humans, Drug Metabolism and Disposition. 27 (1998) 213–220.
[21] L. Di, The Impact of Carboxylesterases in Drug Metabolism and Pharmacokinetics, Curr Drug Metab. 20 (2019) 91–102. https://doi.org/10.2174/1389200219666180821094502.
[22] M. Hosokawa, Structure and Catalytic Properties of Carboxylesterase Isozymes Involved in Metabolic Activation of Prodrugs, Molecules. 13 (2008) 412–431. https://doi.org/10.3390/molecules13020412.

[23] B. Li, M. Sedlacek, I. Manoharan, R. Boopathy, E.G. Duysen, P. Masson, O. Lockridge, Butyrylcholinesterase, paraoxonase, and albumin esterase, but not carboxylesterase, are present in human plasma, Biochemical Pharmacology. 70 (2005) 1673–1684. https://doi.org/10.1016/j.bcp.2005.09.002.
[24] C. Ohnmacht, M. Cooley, R. Darling, S. Lei, V. Patel, Sample stabilization strategies: a case study review of unique sample collection and handling procedures, Bioanalysis. 11 (2019) 1867–1880. https://doi.org/10.4155/bio-2019-0238.
[25] N. Lindegardh, G.R. Davies, T.T. Hien, J. Farrar, P. Singhasivanon, N.P.J. Day, N.J. White, Rapid Degradation of Oseltamivir Phosphate in Clinical Samples by Plasma Esterases, Antimicrob Agents Chemother. 50 (2006) 3197–3199. https://doi.org/10.1128/AAC.00500-06.
[26] X.-L. Wei, R. Han, X. Hu, L.-H. Quan, C.-Y. Liu, Q. Chang, Y.-H. Liao, Stabilization of zeylenone in rat plasma by the presence of esterase inhibitors and its LC-MS/MS assay for pharmacokinetic study, Biomedical Chromatography. 27 (2013) 636–640. https://doi.org/10.1002/bmc.2838.
[27] S.K. Dp, P. C, S.R. Jvln, DEVELOPMENT AND VALIDATION OF A DRIED BLOOD SPOT LC-MS/MS ASSAY TO QUANTIFY GEMCITABINE IN HUMAN WHOLE BLOOD: A COMPARISION WITH AND WITHOUT CYTIDINE DEAMINASE INHIBITOR, International Journal of Pharmacy and Pharmaceutical Sciences. (2015) 75–81.
[28] W.F. Lavallee, H. Rosenkrantz, Evidence for pilocarpine transformation by serum, Biochemical Pharmacology. 15 (1966) 206–210. https://doi.org/10.1016/0006-2952(66)90064-5.
[29] J. Li, S. Xu, Y. Peng, N. Feng, L. Wang, X. Wang, Conversion and pharmacokinetics profiles of a novel pro-drug of 3- n -butylphthalide, potassium 2-(1-hydroxypentyl)-benzoate, in rats and dogs, Acta Pharmacologica Sinica. 39 (2018) 275–285. https://doi.org/10.1038/aps.2017.90.
[30] F. Gil, M.C. Gonzalvo, A.F. Hernandez, E. Villanueva, A. Pla, Differences in the kinetic properties, effect of calcium and sensitivity to inhibitors of paraoxon hydrolase activity in rat plasma and microsomal fraction from rat liver, Biochemical Pharmacology. 48 (1994) 1559–1568. https://doi.org/10.1016/0006-2952(94)90200-3.
[31] F.A. de Jong, R.H.J. Mathijssen, P. de Bruijn, W.J. Loos, J. Verweij, A. Sparreboom, Determination of irinotecan (CPT-11) and SN-38 in human whole blood and red blood cells by liquid chromatography with fluorescence detection, Journal of Chromatography B. 795 (2003) 383–388. https://doi.org/10.1016/S1570-0232(03)00574-9.
[32] E. Tsakalozou, J. Horn, M. Leggas, An HPLC Assay for the Lipophilic Camptothecin Analog AR-67 Carboxylate and Lactone in Human Whole Blood, Biomed Chromatogr. 24 (2010) 1045–1051. https://doi.org/10.1002/bmc.1404.
[33] A. van Veelen, R. van Geel, Y. de Beer, A.-M. Dingemans, L. Stolk, R. ter Heine, F. de Vries, S. Croes, Validation of an analytical method using HPLC–MS/MS to quantify osimertinib in human plasma and supplementary stability results, Biomedical Chromatography. 34 (2020) e4771. https://doi.org/10.1002/bmc.4771.
[34] T. Tai, H. Zhou, T. Zhu, Y.-M. Jia, J.-Z. Ji, Y.-F. Li, Q.-Y. Mi, H.-G. Xie, Development and validation of a UPLC–MS/MS method for simultaneous determination of vicagrel and its major metabolites in rat or human plasma: An optimized novel strategy for the stabilization of vicagrel, Journal of Pharmaceutical and Biomedical Analysis. 179 (2020) 112955. https://doi.org/10.1016/j.jpba.2019.112955.

[35] L. Di, E.H. Kerns, Y. Hong, H. Chen, Development and application of high throughput plasma stability assay for drug discovery, International Journal of Pharmaceutics. 297 (2005) 110–119. https://doi.org/10.1016/j.ijpharm.2005.03.022.
[36] R.L. Lalonde, K.G. Kowalski, M.M. Hutmacher, W. Ewy, D.J. Nichols, P.A. Milligan, B.W. Corrigan, P.A. Lockwood, S.A. Marshall, L.J. Benincosa, T.G. Tensfeldt, K. Parivar, M. Amantea, P. Glue, H. Koide, R. Miller, Model-based Drug Development, Clinical Pharmacology & Therapeutics. 82 (2007) 21–32. https://doi.org/10.1038/sj.clpt.6100235.
[37] A.Z. Zhu, Quantitative translational modeling to facilitate preclinical to clinical efficacy & toxicity translation in oncology, Future Science OA. 4 (2018) FSO306. https://doi.org/10.4155/fsoa-2017-0152.
[38] P. Ratnatilaka Na Bhuket, P. Jithavech, B. Ongpipattanakul, P. Rojsitthisak, Interspecies differences in stability kinetics and plasma esterases involved in hydrolytic activation of curcumin diethyl disuccinate, a prodrug of curcumin, RSC Advances. 9 (2019) 4626–4634. https://doi.org/10.1039/C8RA08594C.
[39] L. Berry, L. Wollenberg, Z. Zhao, Esterase Activities in the Blood, Liver and Intestine of Several Preclinical Species and Humans, Drug Metabolism Letters. 3 (2009) 70–77. https://doi.org/10.2174/187231209788654081.
[40] P. Bouyssou, C.L. Goff, J. Chenault, Synthesis of 7- and 5,7-substituted-6-fluoro-2-methyl-1,2,3,4-tetrahydroquinolines: Convenient precursors of quinolone antibacterial agents, Journal of Heterocyclic Chemistry. 29 (1992) 895–898. https://doi.org/10.1002/jhet.5570290436.
[41] Guideline on Bioanalytical Method Validation, European Medicines Agency. (2011). https://www.ema.europa.eu/en/documents/scientific-guideline/guideline-bioanalytical-method-validation_en.pdf.
[42] P. Hubert, J. Nguyenhuu, B. Boulanger, E. Chapuzet, P. Chiap, N. Cohen, P. Compagnon, W. Dewe, M. Feinberg, M. Lallier, Harmonization of strategies for the validation of quantitative analytical procedures. A SFSTP proposal—part I, Journal of Pharmaceutical and Biomedical Analysis. 36 (2004) 579–586. https://doi.org/10.1016/S0731-7085(04)00329-2.
[43] Ph. Hubert, J.-J. Nguyen-Huu, B. Boulanger, E. Chapuzet, P. Chiap, N. Cohen, P.-A. Compagnon, W. Dewé, M. Feinberg, M. Lallier, M. Laurentie, N. Mercier, G. Muzard, C. Nivet, L. Valat, E. Rozet, Harmonization of strategies for the validation of quantitative analytical procedures. A SFSTP proposal—part II, Journal of Pharmaceutical and Biomedical Analysis. 45 (2007) 70–81. https://doi.org/10.1016/j.jpba.2007.06.013.
[44] Ph. Hubert, J.-J. Nguyen-Huu, B. Boulanger, E. Chapuzet, N. Cohen, P.-A. Compagnon, W. Dewé, M. Feinberg, M. Laurentie, N. Mercier, G. Muzard, L. Valat, E. Rozet, Harmonization of strategies for the validation of quantitative analytical procedures. A SFSTP proposal—part III, Journal of Pharmaceutical and Biomedical Analysis. 45 (2007) 82–96. https://doi.org/10.1016/j.jpba.2007.06.032.
[45] B. Toussaint, F. Lanternier, C. Woloch, D. Fournier, M. Launay, E. Billaud, E. Dannaoui, O. Lortholary, V. Jullien, An ultra performance liquid chromatography-tandem mass spectrometry method for the therapeutic drug monitoring of isavuconazole and seven other antifungal compounds in plasma samples, Journal of Chromatography B. 1046 (2017) 26–33. https://doi.org/10.1016/j.jchromb.2017.01.036.

[46] Q. Yang, R. Moulder k, M.S. Cohen, S. Cai, L.M. Forrest, Cabozantinib Loaded DSPE-PEG2000 Micelles as Delivery System: Formulation, Characterization and Cytotoxicity Evaluation, BAOJ Pharm Sci. 1 (2015) 001.
[47] B. Heurtault, P. Saulnier, B. Pech, J.-E. Proust, J.-P. Benoit, A novel phase inversion-based process for the preparation of lipid nanocarriers, Pharm. Res. 19 (2002) 875–880.
[48] K.-H. Diehl, R. Hull, D. Morton, R. Pfister, Y. Rabemampianina, D. Smith, J.-M. Vidal, C.V.D. Vorstenbosch, A good practice guide to the administration of substances and removal of blood, including routes and volumes, Journal of Applied Toxicology. 21 (2001) 15–23. https://doi.org/10.1002/jat.727.
[49] A.P. Bolliger, N. Everds, Haematology of the Mouse, in: The Laboratory Mouse, Elsevier, 2012: pp. 331–347. https://doi.org/10.1016/B978-0-12-382008-2.00014-3.
[50] F.G. Bahar, K. Ohura, T. Ogihara, T. Imai, Species Difference of Esterase Expression and Hydrolase Activity in Plasma, Journal of Pharmaceutical Sciences. 101 (2012) 3979–3988. https://doi.org/10.1002/jps.23258.
[51] C.M. Seibert, F.M. Raushel, Structural and Catalytic Diversity within the Amidohydrolase Superfamily, Biochemistry. 44 (2005) 6383–6391. https://doi.org/10.1021/bi047326v.
[52] M.I. Mackness, Human Serum Paraoxonase Is Inhibited in EDTA Plasma, Biochemical and Biophysical Research Communications. 242 (1998) 249. https://doi.org/10.1006/bbrc.1997.7872.
[53] A. Tvarijonaviciute, F. Tecles, M. Caldin, S. Tasca, J. Cerón, Validation of spectrophotometric assays for serum paraoxonase type-1 measurement in dogs, 73 (2012) 8.
[54] T. Minagawa, Y. Kohno, T. Suwa, A. Tsuji, Species differences in hydrolysis of isocarbacyclin methyl ester (TEI-9090) by blood esterases, Biochemical Pharmacology. 49 (1995) 1361–1365. https://doi.org/10.1016/0006-2952(95)00071-7.
[55] S. Yamaori, N. Fujiyama, M. Kushihara, T. Funahashi, T. Kimura, I. Yamamoto, T. Sone, M. Isobe, T. Ohshima, K. Matsumura, M. Oda, K. Watanabe, Involvement of Human Blood Arylesterases and Liver Microsomal Carboxylesterases in Nafamostat Hydrolysis, Drug Metabolism and Pharmacokinetics. 21 (2006) 147–155. https://doi.org/10.2133/dmpk.21.147.
[56] S.J. Kelly, D.E. Dardinger, L.G. Butler, Hydrolysis of phosphonate esters catalyzed by 5'-nucleotide phosphodiesterase, Biochemistry. 14 (1975) 4983–4988. https://doi.org/10.1021/bi00693a030.
[57] R.M. Wadkins, J.L. Hyatt, X. Wei, K.J.P. Yoon, M. Wierdl, C.C. Edwards, C.L. Morton, J.C. Obenauer, K. Damodaran, P. Beroza, M.K. Danks, P.M. Potter, Identification and Characterization of Novel Benzil (Diphenylethane-1,2-dione) Analogues as Inhibitors of Mammalian Carboxylesterases, J. Med. Chem. 48 (2005) 2906–2915. https://doi.org/10.1021/jm049011j.
[58] S.A. Kardos, Interactions of the Organophosphates Paraoxon and Methyl Paraoxon with Mouse Brain Acetylcholinesterase, Toxicological Sciences. 58 (2000) 118–126. https://doi.org/10.1093/toxsci/58.1.118.
[59] A.A. Kousba, Comparison of Chlorpyrifos-Oxon and Paraoxon Acetylcholinesterase Inhibition Dynamics: Potential Role of a Peripheral Binding Site, Toxicological Sciences. 80 (2004) 239–248. https://doi.org/10.1093/toxsci/kfh163.
[60] C.A. Rosenfeld, L.G. Sultatos, Concentration-Dependent Kinetics of Acetylcholinesterase Inhibition by the Organophosphate Paraoxon, Toxicological Sciences. 90 (2006) 460–469. https://doi.org/10.1093/toxsci/kfj094.

[61] W. Xie, P.J. Wilder, J. Stribley, A. Chatonnet, A. Rizzino, P. Taylor, S.H. Hinrichs, O. Lockridge, Knockout of one acetylcholinesterase allele in the mouse, Chemico-Biological Interactions. 119–120 (1999) 289–299. https://doi.org/10.1016/S0009-2797(99)00039-3.

Table 1.

Concentrations (µg/mL) for the eight calibration standards, the six quality controls in human plasma, and the three quality controls in mouse plasma.

Sample type	Number of levels	[CE3F4] for each level (µg/mL)							
Calibration	8	0.40	0.97	2.36	5.74	13.9	33.9	82.3	200
Human quality controls	6	0.40	1.50	5.00	25.0	60.0	150		
Murine quality controls	3	0.40	8.00	150					

Table 2.

Detail of volumes (µL) used for the sample preparation, for each working solution (calibration standard, CS; and human or murine quality control, QC), plasma (human or murine), and solvents.

Sample type	CS	QC	Plasma with unknown [(*R*)-CE3F4]	Blank plasma	EtOH	ACN for extraction
Calibration	50	-	-	50	-	150
QC	-	50	-	-	50	150
Plasma samples (human or murine)	-	-	50	-	50	150

Table 3.

Average parameters of the linear regression obtained from three calibration curves of the analytes with a 1/concentration² weighting at 220 or 250 nm.

Wavelength	n	Linear range	R² (±SD)	Slope (±SD)	y-Intercept (±SD)
220 nm	3	0.40-200 µg/mL	0.9967 (±0.0008)	14585.5 (±773.1)	713.1 (±987.6)
250 nm	3	0.40-200 µg/mL	0.9972 (±0.0025)	4136.7 (±113.7)	-174.1 (±143.6)

Table 4.

Within -day and between days accuracies and precisions on six quality control for quantification at 220 nm (A) and 250 nm (B). CV: coefficient of variation.

(A)	QC level	QC1	QC2	QC3	QC4	QC5	QC6
Within-day accuracy (%), n = 5 per day	Day 1	7.35	-1.46	-4.56	-8.12	0.49	5.11
	Day 2	4.17	-6.98	-7.76	-12.22	-5.13	-2.31
	Day 3	2.10	1.67	-2.56	-6.29	1.52	2.41
Within-day CV (%)		7.95	3.20	3.02	2.26	2.55	2.44
Between-days accuracy (%), n = 3		17.00	-2.94	-9.21	-11.88	-5.01	1.93
Between-days CV (%)		5.01	10.38	3.08	2.99	2.54	6.64
(B)	QC level	QC1	QC2	QC3	QC4	QC5	QC6
Within-day accuracy (%), n = 5 per day	Day 1	5.18	1.28	-4.49	-9.69	-1.43	2.94
	Day 2	9.84	-6.86	-6.39	-8.32	-0.50	2.65
	Day 3	4.80	1.88	-2.46	-5.89	3.10	4.19
Within-day CV (%)		8.86	3.72	3.06	2.18	2.42	2.26
Between-days accuracy (%), n = 3		19.20	2.74	-7.42	-11.03	-1.07	5.15
Between-days CV (%)		6.01	9.41	3.44	2.61	5.62	0.72

Table 5.

Stability of (*R*)-CE3F4 in mouse plasma sample in presence of enzyme inhibitors BNPP or benzil.

Time (h)	[BNPP] (M)			[Benzil] (M)		
	10^{-4}	10^{-5}	10^{-6}	10^{-4}	10^{-5}	10^{-6}
0	100%	100,00%	100,00%	100,00%	100,00%	100,00%
0,5	68,2%	67,7%	56,1%	56,8%	60,4%	59,4%
1	56,6%	41,8%	37,6%	33,7%	35,2%	36,4%

Table 6.

Average parameters of the linear regression obtained from three calibration curves of the analytes with a 1/concentration² weighting at 220 or 250 nm.

Wavelength	n	Linear range	R^2 (±SD)	Slope (±SD)	y-Intercept (±SD)
250 nm	3	0.40-200 µg/mL	0.9964 (±0.0015)	5339.8 (±90.0)	-93.0 (±184.1)

Table 7.

Within-day and between days accuracies and precisions on three quality control for quantification at 250 nm in murine plasma. CV: coefficient of variation.

	QC level	QC1	QC2	QC3
Within-day accuracy (%), n = 5 per day	Day 1	-3.93	-6.40	-7.40
	Day 2	0.78	-7.70	-9.71
	Day 3	-2.14	-2.13	-7.80
Within-day CV (%)		4.30	4.37	1.08
Between-days accuracy (%), n = 3		-4.11	-2.68	-9.65
Between-days CV (%)		7.68	10.23	1.82

Table 8.

Apparent half-life in murine plasma at 37°C of the (*R*)-CE3F4 in different formulations.

Formulation	Apparent half-life (h)
DSPE-PEG_{2000} micelles	0.8
Solutol HS 15 & PEG_{200} mixture	2.7
Lipid nanocapsules	5.5

Figure caption

Figure 1.

Structure of (*R*)-CE3F4.

Figure 2.

Chromatograms of blank human plasma extract at 220 nm (A) and 250 nm (B).

Figure 3.

Chromatograms of blank mouse plasma extract at 220 nm (A) and 250 nm (B)

Figure 4.

Chromatograms at 220 nm (A) and 250 nm (A') of (*R*)-CE3F4 (TR = 4.2 min) and its principal metabolite (TR = 8.6 min) in murine plasma, after 3h at 37°C. Chromatograms at 220 nm (B) and 250 nm (B') in human plasma, after 24h at 37°C.

Figure 5.

(A) Kinetics of the disappearance of the (*R*)-CE3F4 based on signal variation in human (at 220 nm) or murine (at 250 nm) plasma. Continuous lines represent the mean regression and the dotted lines represent the confidence interval on the regression (95%). (B) Kinetics of the principal metabolite of the (*R*)-CE3F4 (TR = 8.6 min) observed at 250 nm in murine and human plasma at 37°C.

Figure 6.

Effect of paraoxon on (*R*)-CE3F4 metabolism in murine plasma at 37°C. Paraoxon was at different concentrations added 10 minutes before the addition of (*R*)-CE3F4 (blue, orange, and red lines), or simultaneously (green line).

Figure 7.

Chromatograms of (A) murine plasma sample containing (*R*)-CE3F4 and metabolite, (B) (*R*)-CE3F4 at 5 µg/mL, and (C) deformylated-CE3F4 at 5 µg/mL. Total ion chromatogram is presented as a continuous black line, extracted ion chromatogram of m/z 351.9 is presented as

a dotted red line, and extracted ion chromatogram of m/z 323.9 is presented as a dotted blue line.

Figure 8.

MS spectrum extracted at 18.3 min, isotopic distribution of m/z 323.9 and MS/MS spectrum of the parent ion m/z 323.9, in plasma sample (A, C and E respectively) and a control sample of deformylated-CE3F4 (B, D, and F respectively).

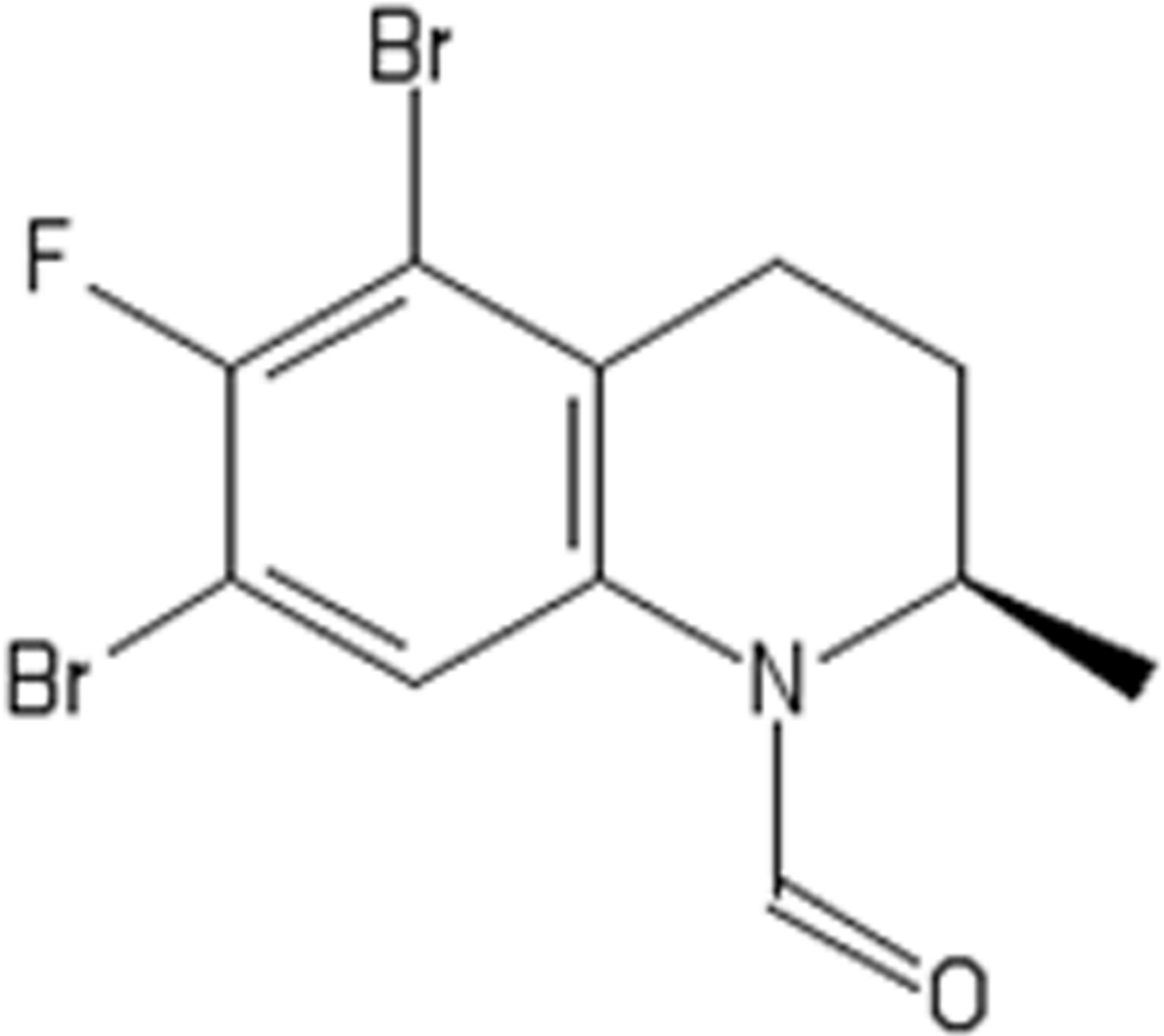
Br
F
Br
N
O

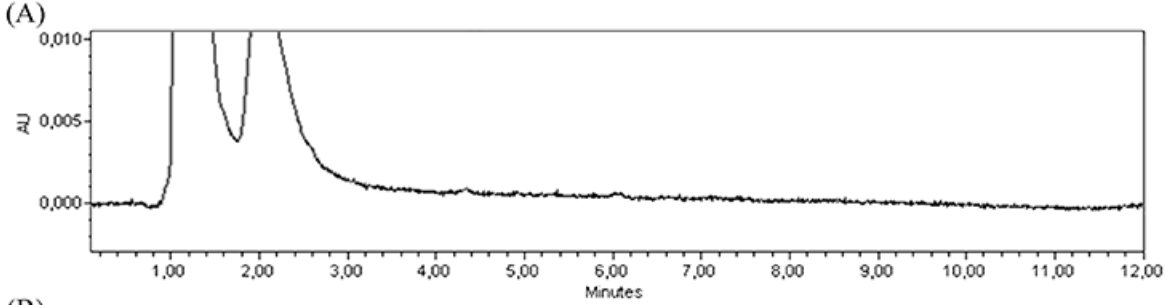
(A)
0,010
0,005
0,000
AU
1,00
2,00
3,00
4,00
5,00
6,00
7,00
8,00
9,00
10,00
11,00
12,00
Minutes
(B)
0,010
0,005
0,000
AU
1,00
2,00
3,00
4,00
5,00
6,00
7,00
8,00
9,00
10,00
11,00
12,00
Minutes

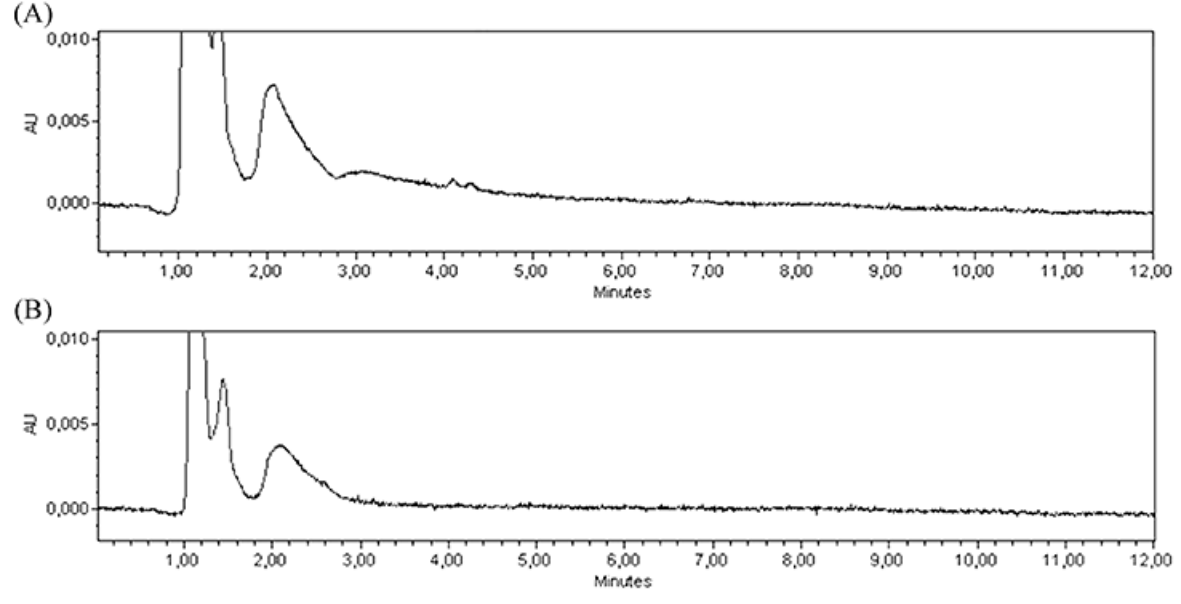
(A)
0,010
0,005
0,000
AU
1,00
2,00
3,00
4,00
5,00
6,00
7,00
8,00
9,00
10,00
11,00
12,00
Minutes
(B)
0,010
0,005
0,000
AU
1,00
2,00
3,00
4,00
5,00
6,00
7,00
8,00
9,00
10,00
11,00
12,00
Minutes

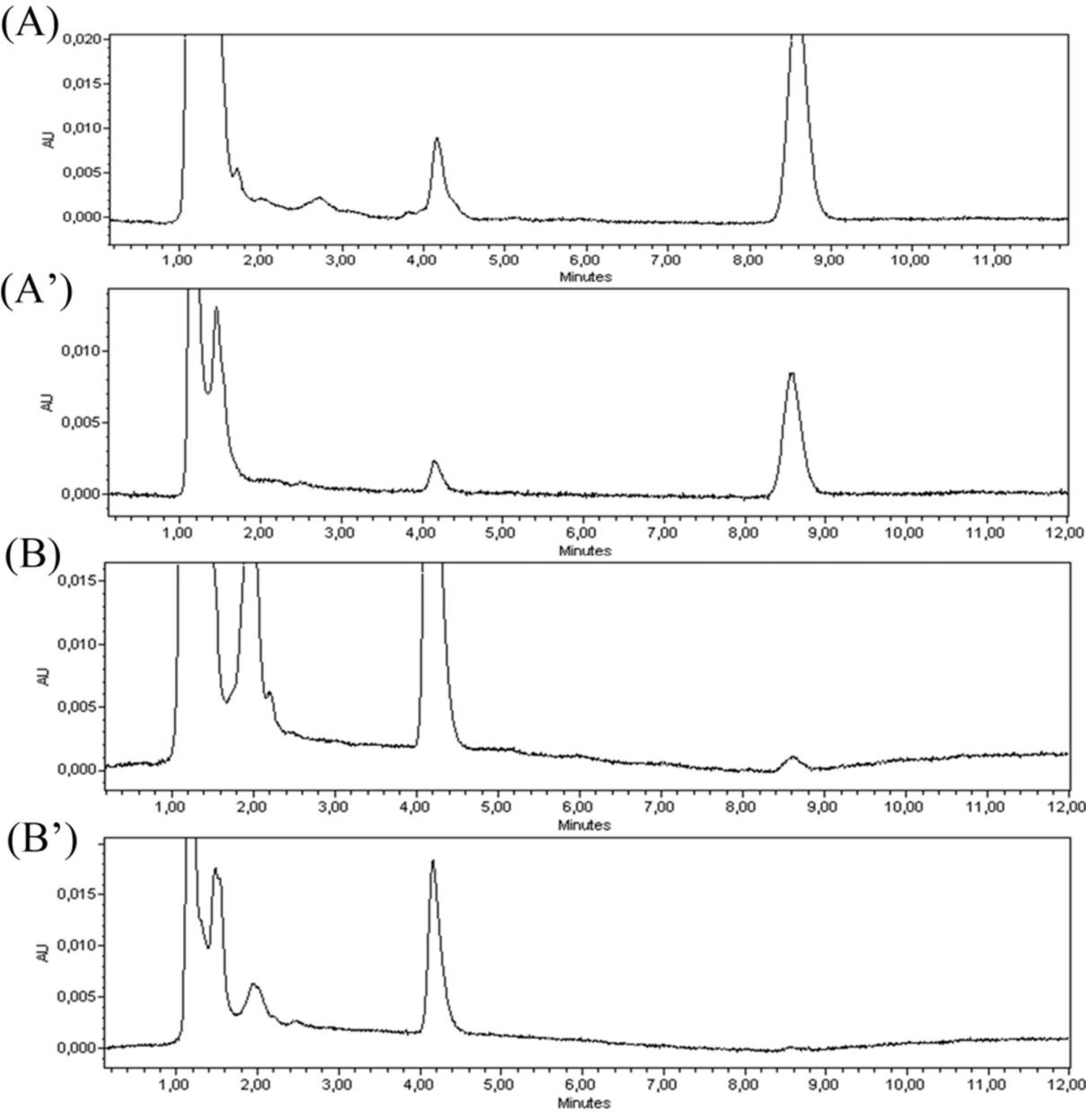
(A)
AU
0,020
0,015
0,010
0,005
0,000
1,00
2,00
3,00
4,00
5,00
6,00
7,00
8,00
9,00
10,00
11,00
Minutes
(A')
AU
0,010
0,005
0,000
1,00
2,00
3,00
4,00
5,00
6,00
7,00
8,00
9,00
10,00
11,00
12,00
Minutes
(B)
AU
0,015
0,010
0,005
0,000
1,00
2,00
3,00
4,00
5,00
6,00
7,00
8,00
9,00
10,00
11,00
12,00
Minutes
(B')
AU
0,015
0,010
0,005
0,000
1,00
2,00
3,00
4,00
5,00
6,00
7,00
8,00
9,00
10,00
11,00
12,00
Minutes

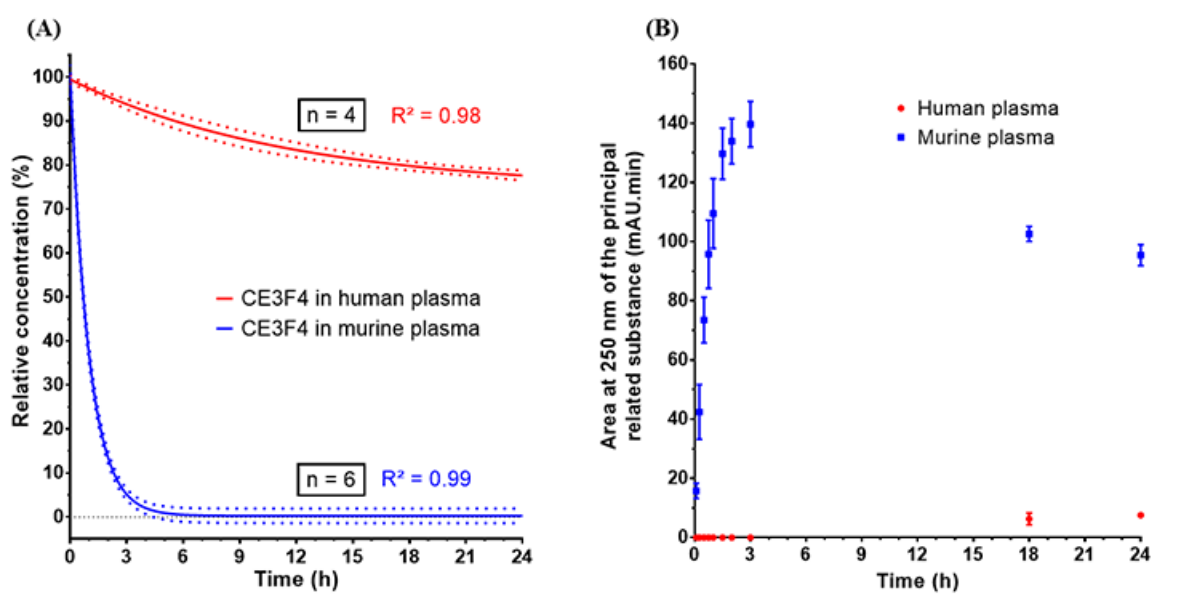
(A)
Relative concentration (%)
Time (h)
n = 4
R² = 0.98
n = 6
R² = 0.99
CE3F4 in human plasma
CE3F4 in murine plasma
(B)
Area at 250 nm of the principal related substance (mAU.min)
Time (h)
Human plasma
Murine plasma

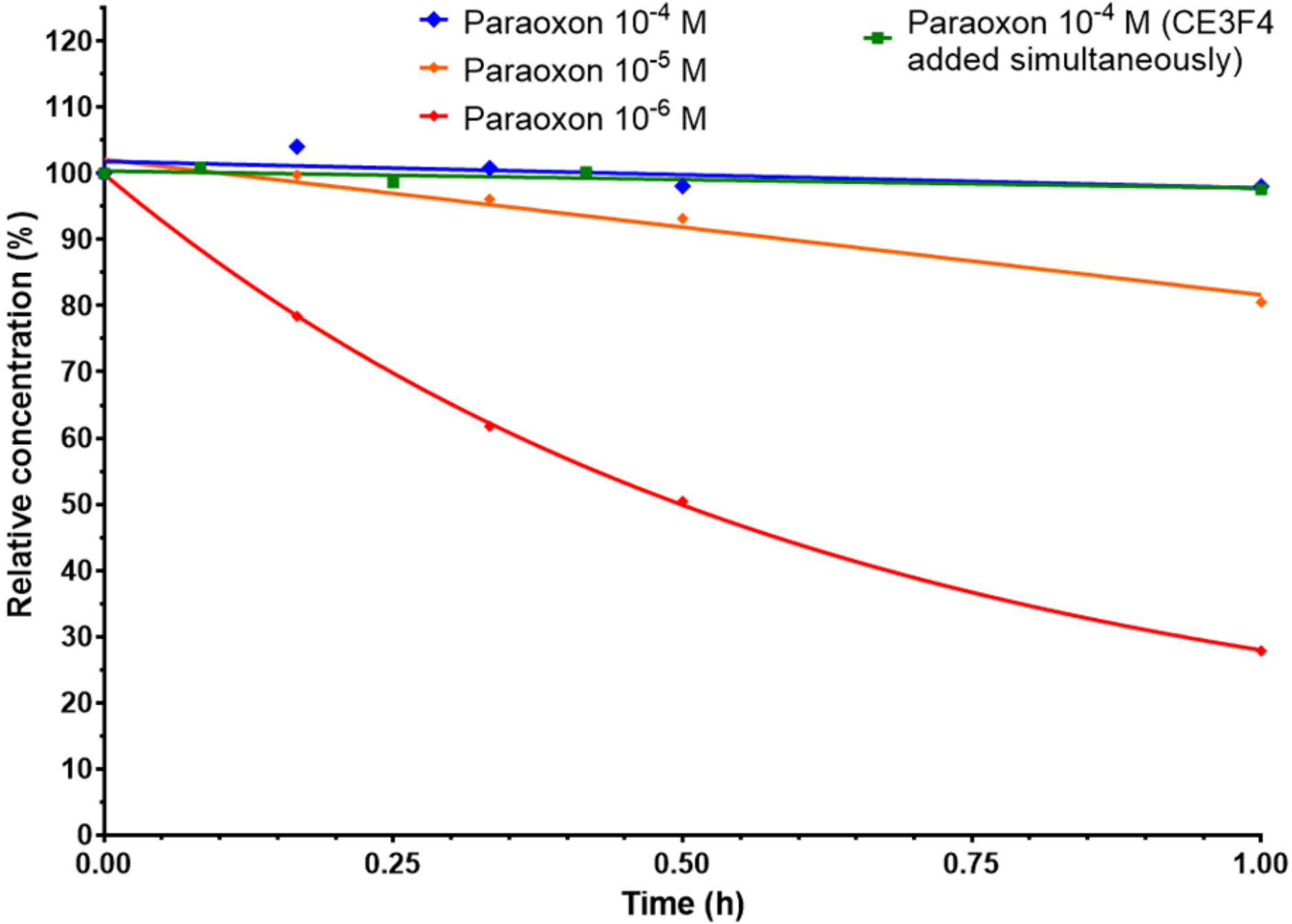
Paraoxon 10-4 M
Paraoxon 10-5 M
Paraoxon 10-6 M
Paraoxon 10-4 M (CE3F4 added simultaneously)
Relative concentration (%)
Time (h)
0
10
20
30
40
50
60
70
80
90
100
110
120
0.00
0.25
0.50
0.75
1.00

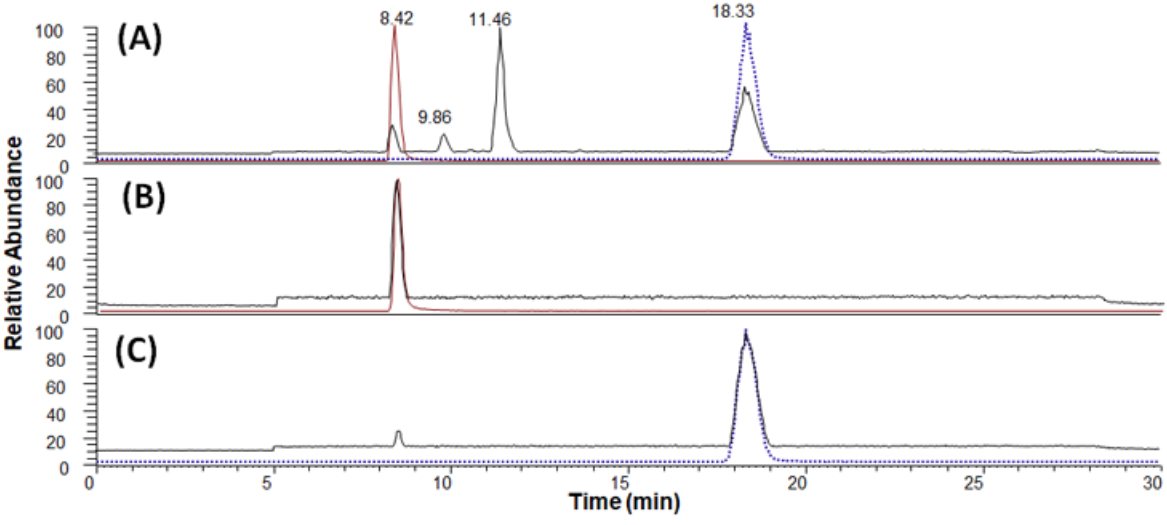
(A)
(B)
(C)
8.42
9.86
11.46
18.33
Relative Abundance
Time (min)
0
20
40
60
80
100
0
5
10
15
20
25
30

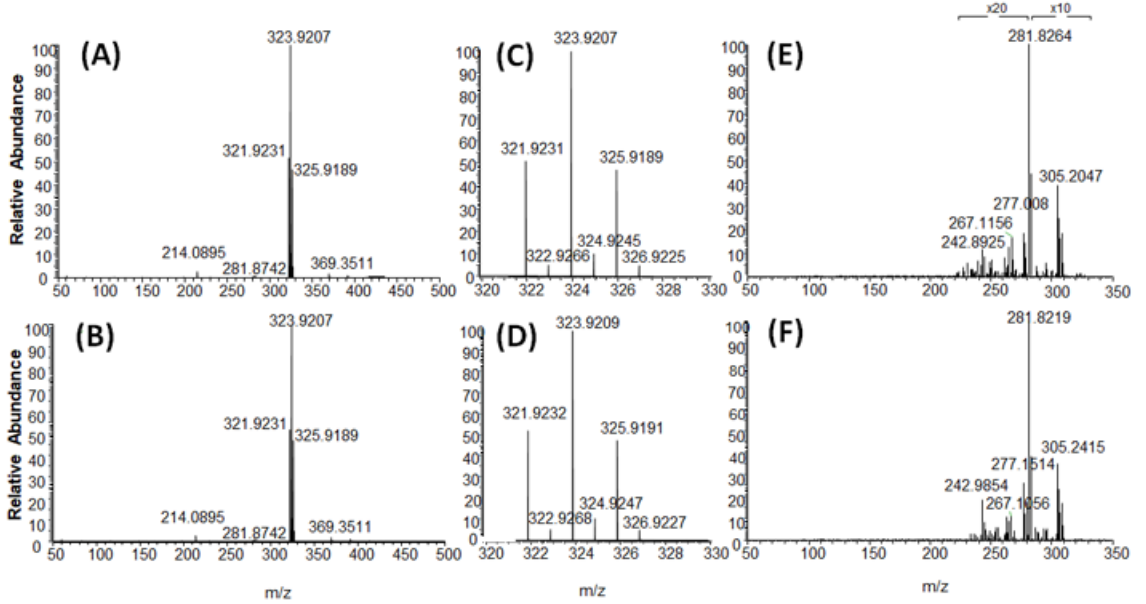
(A)
323.9207
321.9231
325.9189
214.0895
281.8742
369.3511
(B)
323.9207
321.9231
325.9189
214.0895
281.8742
369.3511
(C)
323.9207
321.9231
325.9189
322.9266
324.9245
326.9225
(D)
323.9209
321.9232
325.9191
322.9268
324.9247
326.9227
(E)
x20
x10
281.8264
305.2047
277.008
267.1156
242.8925
(F)
281.8219
305.2415
277.1514
242.9854
267.1156
Relative Abundance
m/z